The International Journal of Advanced Manufacturing Technology (2018) 99:1603–1613
https://doi.org/10.1007/s00170-018-2552-2

ORIGINAL ARTICLE

Improving weld penetration by employing of magnetic poles' configurations to an autogenous tungsten inert gas (TIG) welding

Ario Sunar Baskoro[1] · Angga Fauzian[1] · Haikal Basalamah[1] · Gandjar Kiswanto[1] · Winarto Winarto[2]

Received: 12 December 2017 / Accepted: 12 August 2018 / Published online: 24 August 2018

Abstract
A new configuration of permanent magnet as a source of external magnetic field has been established to an autogenous tungsten inert gas (TIG) welding. The external magnetic field is generated by rectangle shape NdFeB permanent magnets of 260 mT and arranged in cups-type magnetic field (CMF). A charge-coupled device (CCD) is applied to monitor the phenomenon of the arc shape. The material used in this experiment is SS304 with a thickness of 2 mm. This study aims at investigating the effect of external magnetic field towards the arc shape and finding the configuration, which can reduce the power consumption and improve penetration. A significant effect on the improvement of welding efficiency can be achieved by using PR-NNSS-SD (50 or 70 mm), PP-NNSS-SD (70 or 90 mm), or PP-NSNS-Pull (50 mm). These configurations can reduce the power consumption up to 11%.

Keywords Tungsten inert gas (TIG) · External magnetic field · Magnetic poles' configurations · Autogenous · Power efficiency

1 Introduction

Tungsten inert gas (TIG) welding is one of the most widely used manufacturing joint process, such as the auto industry, shipbuilding, and aerospace industry [1]. Although the research related to TIG welding has been matured, the development to improve the effectiveness and performance of the weld process is still going on. An advanced welding technology, which introduces an external magnetic field (EMF) during the welding process, has been proposed in 1962 by Brown et al. In fact, the shape of arc plasma is influenced by the presence of an EMF; this has been proven in many literatures [2]. In general cases, EMF leads to an unbalance of the electromagnetic force generated by the welding current. Hence, it causes a deflection that is called arc blow. Previous studies using numerical approach have demonstrated that the EMF has affected the arc plasma in the process of TIG welding. As a result, the welding arc was not focused on the object and the weld penetration was reduced [3]. Since the existence of EMF has many disadvantages, in many cases, it is avoided in the welding process. However, in some cases, an EMF is applied on purpose to control the arc plasma deflection [4].

Many researchers have attempted with various configurations of pulsed magnetic field or constant magnetic field and generated by induction coil or permanent magnet. Based on various configurations, the magnetic field can be classified cups magnetic field (CMF), axial magnetic field (AMF), longitudinal magnetic field (LMF), transverse magnetic field (TMF), and rotating magnetic field (RMF). Nomura et al. [5] investigated arc shape using small permanent magnets. They produce cups-type magnetic field using four permanent magnets and results in the arc elliptical shape. Baskoro et al. [6] studied the effect of rotating magnetic field to the arc shape and the weld width. The magnetic field was generated by eight induction coil that are activated sequentially. Sun et al. [7] employing double EMF poles and investigated the effect of magnetic field frequency and magnetic flux density on the arc shape, sidewall penetration, and weld penetration. Double magnetic pole produces a uniform distribution of magnetic lines and resulted in enhancing magnetic flux density and also increased the side wall penetration. Recently, Liu et al. [8] show that the implementation of LMF could drive particles to rotate and expand the arc. Blais et al. [9] use wire as a conductor to deflect the arc and

✉ Ario Sunar Baskoro
ario@eng.ui.ac.id

[1] Department of Mechanical Engineering, Faculty of Engineering, Universitas Indonesia, Kampus Baru UI Depok, Depok 16424, Indonesia

[2] Department of Metallurgical and Materials Engineering, Faculty of Engineering, Universitas Indonesia, Kampus Baru UI Depok, Depok 16424, Indonesia

study the phenomenon using numerical and experimental. This wire acts like transverse magnetic field (TMF). Lin et al. [10] studied effect of external longitudinal magnetic field (LMF) on the arc weld pool. Li et al. [11] and Chen et al. [12] focused on the effect of axial magnetic field (AMF) using DC source. Another researcher focused on TMF [7, 13, 14], LMF [8, 15], CMF [5, 6], AMF [3], and RMF [1].

Many researchers have studied numerical approach for developing three-dimensional coupled model. Most of them are using coil to generate induction magnetic field and a few researcher attempted using permanent magnet as EMF source. Previous studies [5] found that cups-type arrangement will compress the welding arc and result in an elliptical-shaped arc model. However, they do not discuss the influence of external magnetic field towards the power efficiency. In this paper, a cups-type configuration using permanent magnet was attempting to find the best configuration that can achieve increased power efficiency using autogenous TIG welding using DC source.

2 Experiment methods

The materials used in this study are stainless steel 304 with a thickness of 2 mm. The specimens are cut into a dimension of 80 × 25 × 2 mm. The welding process used a power TIG 2200 AC/DC pulse welding machine. Figure 1 schematically shows the experimental setup of TIG welding and measurement with external magnetic field apparatus. The autogenous welding is performed with or without using external permanent magnet. A charge-coupled device (CCD) camera is employed to monitor the arc shape. Table 1 shows that welding parameters are used in this experiment. A static external magnetic field is generated by rectangle shape NdFeB permanent magnets with a size of 25 × 15 × 3 mm. A gaussmeter is used to measure the magnetic induction intensity; it shows the intensity around 260 mT.

The configuration of the magnetic poles is classified into four types which are NNNN, SSSS, NNSS, and NSNS where N is the north pole and S is the south pole. Distance between magnets in all configurations is 50 mm except NNSS where three types of distance are applied, which are 50, 70, and 90 mm. The NNSS with distance between magnets is divided into three categories based on arc phenomenon, which are side deflection (NNSS SD), forward deflection (NNSS FD), and backward deflection (NNSS BD). The NSNS configuration is divided into two categories which are NSNS Pull and NSNS Press. Where the definition of pull means that the arc is stretched tangential to the welding direction, while press means that the arc is stretched normally to the welding direction. The configuration of magnetic pole surface reference is divided into two categories which are perpendicular (PP) and parallel (PR). Hence, there are 18 types of configuration permanent magnet for design of experiment in this paper. The schematic arrangements of external permanent magnet are shown in Fig. 2 and Table 2 shows the configuration of magnetic poles. Measurements are performed by measuring the top bead width, back bead width, and deflection of the weld from the weld line. The bead width is measured using vernier

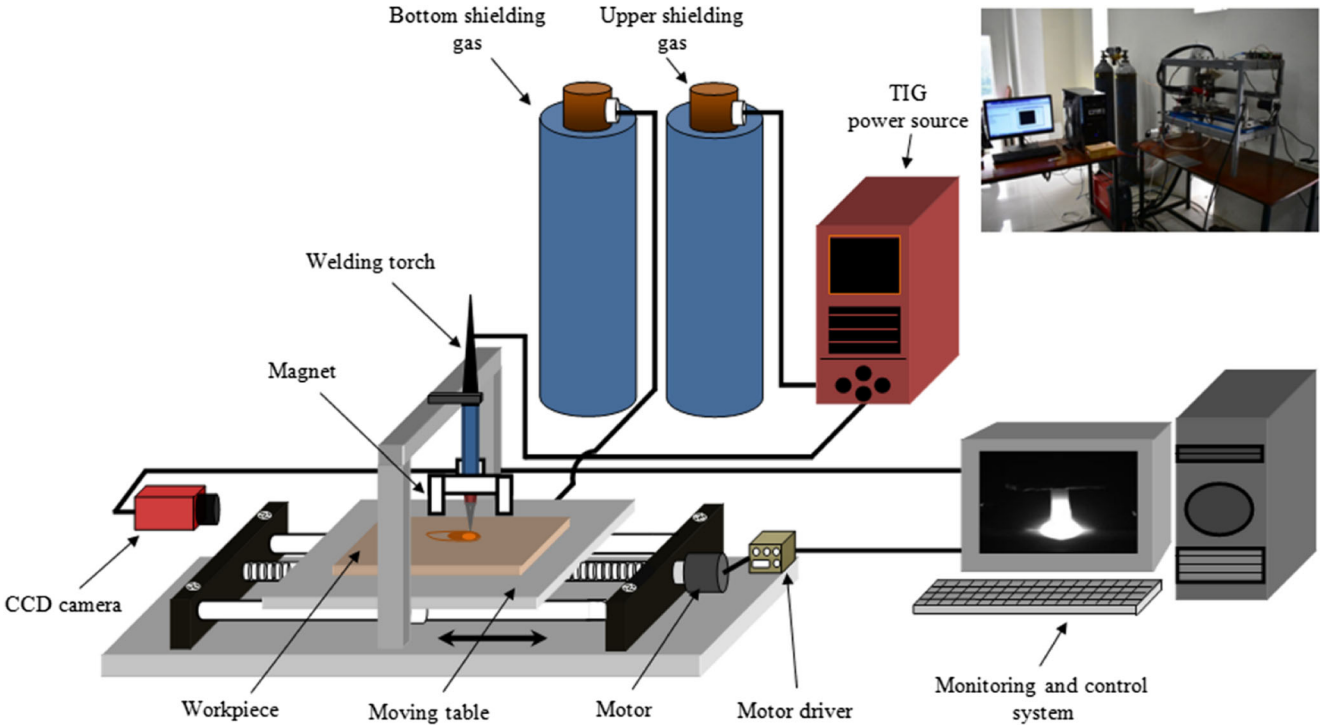

Fig. 1 Schematic illustration of the experimental equipment

Table 1 Welding conditions used in the experiment

Parameter	Unit	Value
Power source	Dimensionless	DCEN
Welding current (I)	A	80, 90
Welding speed (v)	mm/s	2
AWS classification	Dimensionless	E W Th-2
Electrode diameter (d)	mm	2.4
Nominal arc length (h)	mm	2
Shielding gas	Dimensionless	100% Ar
Upper shielding gas flow rate (Q_u)	L/min	10
Bottom shielding gas flow rate (Q_b)	L/min	3

caliper in eight locations and measured from 10 mm at the beginning of the weld bead and the overall value is averaged. Figure 3 illustrates the schematic of measurement of the deflection of the weld lines due to the effect of EMF.

3 Model for external magnetic field

Based on the arrangement of static permanent magnetic field apparatus model, it needs to establish a 2D FEM model to map the direction and distribution of magnetic field and magnitude. The main consideration is the influence of external permanent magnetic field to generate the electromagnetic force and changing the shape of the arc welding. The magnetic field of a permanent magnet can be derived from the vector potential equation:

$$\vec{\boldsymbol{B}} = \nabla \times \vec{\boldsymbol{A}} \tag{1}$$

where B is the magnetic flux density (or magnetic field) and A is the magnetic vector potential. The magnetic flux density in the presence of permanent magnet can be described as:

$$\boldsymbol{B} = \mu_o(\boldsymbol{H} + \boldsymbol{M}) \tag{2}$$

where H is the magnetic field intensity, M is the magnetization produced by the permanent magnet, and μo is the permeability of free space. Magnetostatic or the magnetic field is conservative; the second Maxwell's equation can be simplified to:

$$\nabla \cdot \boldsymbol{B} = 0 \tag{3}$$

so a magnetic scalar potential φ as follows:

$$\boldsymbol{H} = -\nabla\varphi \tag{4}$$

Inserting Eqs. (2) and (4) into equation Eq. (3) will obtain:

$$\nabla \cdot (-\nabla\varphi + \boldsymbol{M_o}) = 0 \tag{5}$$

This can be solved using Vizimag 3.18 software to model in 2D Cartesian form. The assumptions condition for the calculation as follows:

- Homogeneous media with uniform permeability μ = 1.1

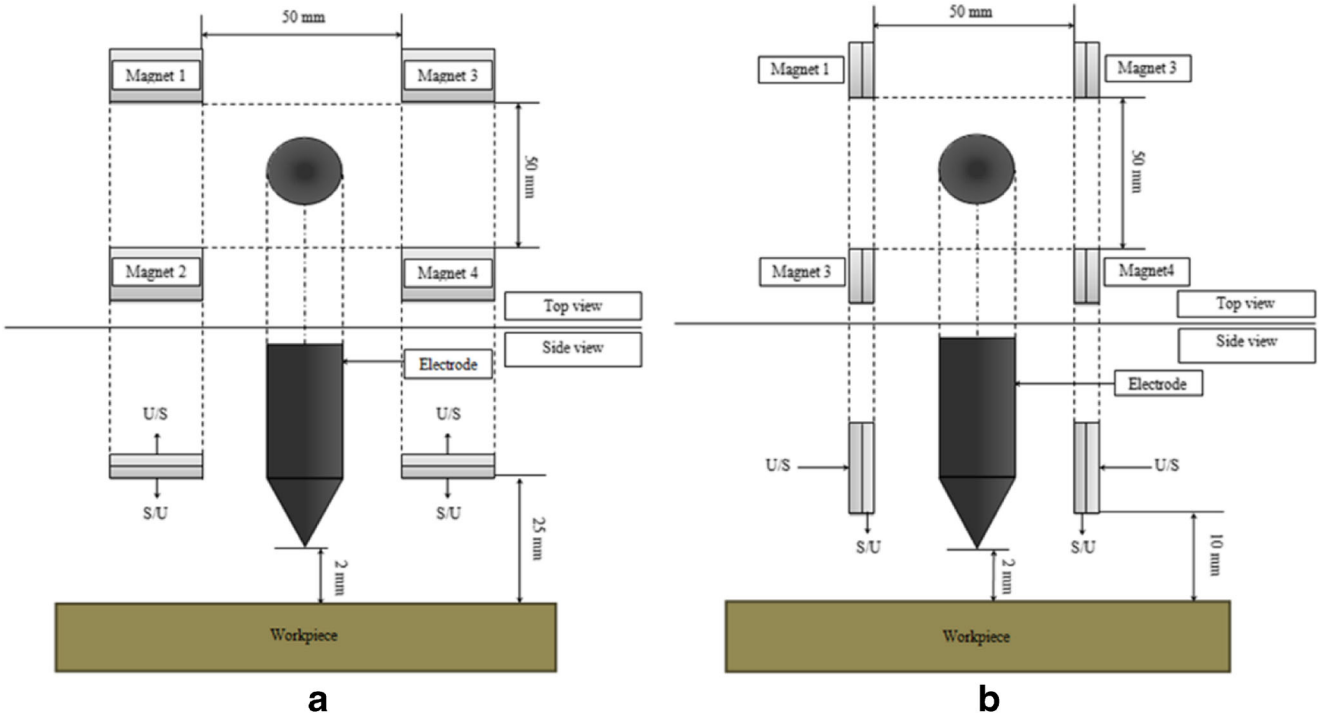

Fig. 2 Schematic experimental set up of magnet arrangement: **a** permanent magnets are arranged parallel (PR) to the workpiece; **b** permanent magnets are arranged perpendicular (PP) to the workpiece

Table 2 Experimental magnet parameters

Position of permanent magnets	Configuration of magnetic poles				Category based on arc phenomenon	Distance between magnets (mm)
Parallel (PR) and perpendicular (PP)	N	S	N	S	Pull and Press	50
	N	N	N	N	–	50
	S	S	S	S	–	50
	N	N	S	S	SD, FD, BD	50
	N	N	S	S	SD	70
	N	N	S	S	SD	90

- No external source except the permanent magnet $\partial B/\partial t = 0$ (magnetostatic case)
- 3rd dimension is neglected

4 Results and discussion

4.1 Effect of EMF on the arc shape

4.1.1 Parallel configuration

As a conservative field (where div$\boldsymbol{B} = 0$), it is essential that the property of the magnetic flux will form a closed loop around the permanent magnets. The loop distribution depends on the position and surface orientation. Figure 4a–c shows the simulation of magnetic field density and the vector direction itself. These three reference cases of surface orientation from the side view are from the parallel (PR) NNSS configuration. As shown in the figure, the color represents the magnitude of $\boldsymbol{B}$, the red color shows the high value of $|\boldsymbol{B}|$, the green shows medium value of $|\boldsymbol{B}|$, and dark blue shows very small value of $|\boldsymbol{B}|$. The flux located on the upper side of the permanent magnet can be neglected because it does not affect the arc, while the flux in the lower side is considered for the main cause to affect the arc shape. Figure 4a shows the side view reference of the magnetic field N-N configuration, Fig. 4b shows the magnetic field of N-S (or S-N) configuration, and Fig. 4c shows the magnetic field of S-S configuration (typically the flux shape is the same as N-N but with opposite direction). The N-N and S-S configurations show the repulsive flux line and turn to make a close loop circle, while N-S (or S-N) configuration shows the attraction flux line.

Figure 5a shows the illustration model for three-dimensional condition. Figure 5b shows the lower side pole reference of magnetic field as the main consideration for the analytical magnetic force on the arc welding. Figure 6a–g shows the predicted magnetic field and magnetic force from cups-type arrangement and the results of the arc shape with all the parallel (PR) configurations. Figure 6a, b shows the NNNN and SSSS configurations that have a magnetic field around the arc that come in for NNNN and come out for SSSS. There is no significant result of the arc shape from this interaction from external magnetic field. According to Wu et al. [2], this is similar to the type of axial magnetic field (AMF) and has a result in a radial force in the arc. Figure 6c, d shows the phenomenon of arc shape that resulted from the configuration of magnets NSNS. There are two terms that indicated the results from NSNS configuration, which are "pull" and "press". Pull means that the arc is stretched tangential to the welding direction; this result will give an elliptical shape of the arc and wider bead width, while press means that the arc is stretched normally to the welding direction and resulted in smaller size bead width. This condition is similar to the longitudinal magnetic field (LMF) that has a result of an elliptical arc shape. Figure 6e–g shows the phenomenon of arc shape that resulted from the configuration of magnets NNSS. There are three terms that indicated the results from NNSS configuration, which are side deflection (SD), forward deflection (FD), and backward deflection (BD). These three cases can be obtained by rotating the NNSS. This condition is similar to the transverse magnetic field (TMF) that has a result of deflecting arc shape.

4.1.2 Perpendicular configuration

Figure 7a–c shows the predicted magnetic field from the side view of three reference cases of the parallel (PR) NNSS

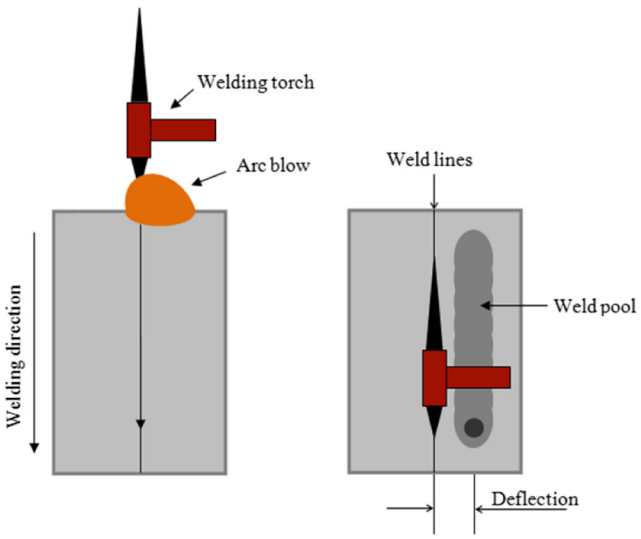

Fig. 3 Schematic illustration of measurement for the deflection of weld lines

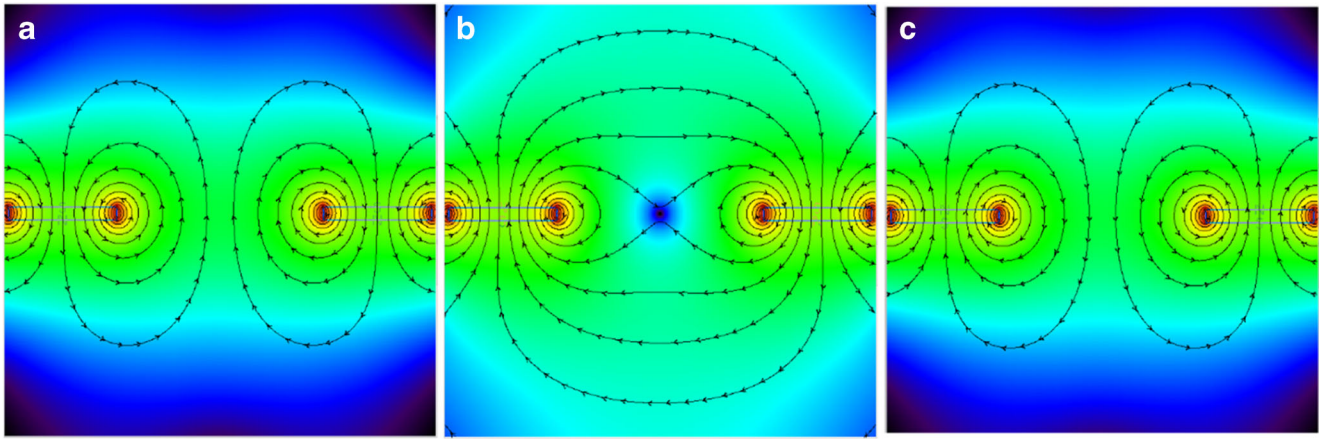

Fig. 4 Two-dimensional simulation of magnetic field density from side view of parallel (PR) configuration, three reference cases: **a** side view reference of the magnetic field N-N configuration; **b** N-S (or S-N) configuration; **c** S-S configuration

configuration. In this case, the flux located in the outer side of the permanent magnet can be neglected because it does not affect the arc, while the flux in the inner side is considered for the main cause to affect the arc shape. The surface orientation of the inner side in each permanent magnets is used for references naming the configuration. Figure 7a shows the magnetic field N-N configuration, Fig. 7b shows the magnetic field of N-S (or S-N) configuration, and Fig. 7c shows the magnetic field of S-S configuration. Figure 8a–g shows the predicted magnetic field and the simulation of magnetic flux density from top view projection. Figure 8a, b shows the arc shape to have an elliptical shape than tends to bend 45° from welding line. Figure 8c shows NSNS Pull, the arc is stretched tangential to the welding direction, while Fig. 8d shows NSNS Press, the arc is stretched tangential to the welding direction. Figure 8e–g shows the arc shape that resulted from the configuration of magnets NNSS. The effects of NNSS of the PR and PP on the arc shape are almost the same, but strong deflection produced by PP. This is resulted by the permanent magnets that are arranged perpendicular (PP) that was stronger than parallel (PR) arrangement. The magnitude

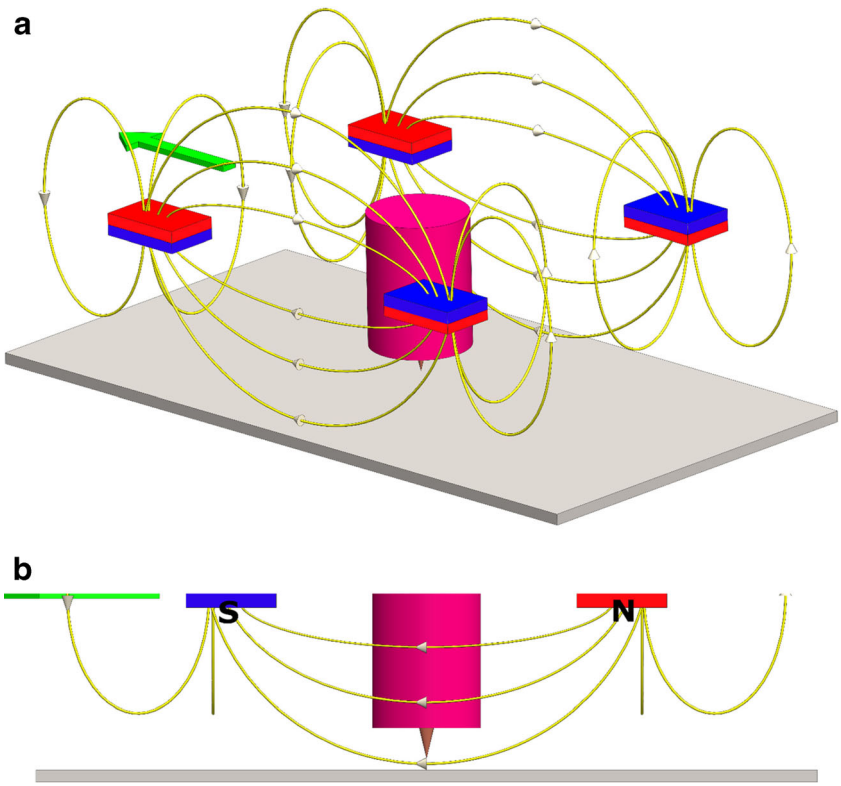

Fig. 5 Schematic illustration model for three-dimensional condition: **a** overall view of 3D; **b** side view of lower side magnetic flux line

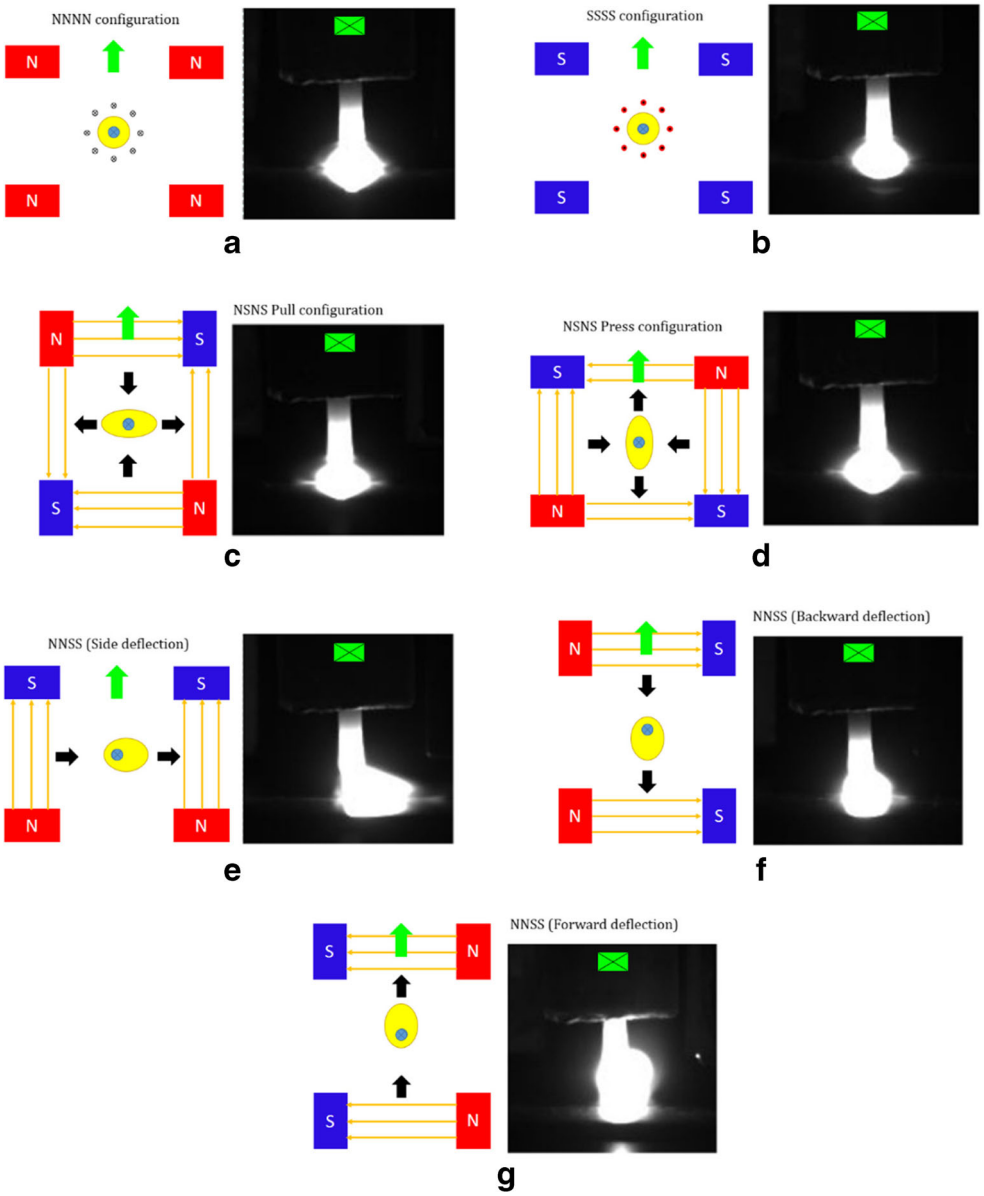

Fig. 6 The illustration of predicted magnetic field with magnetic force from cups-type arrangement and the result of the arc shape in all the parallel (PR) configuration: **a** NNNN; **b** SSSS; **c** NSNS-Pull; **d** NSNS-Press; **e** NNSS-SD; **f** NNSS-BD; **g** NNSS-FD

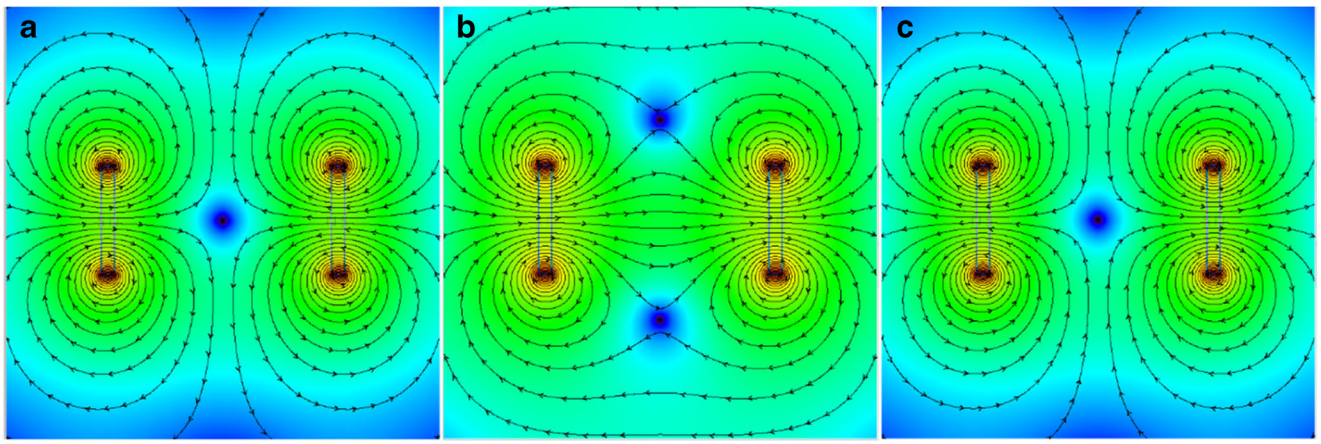

Fig. 7 Two-dimensional simulation of magnetic field density from side view of perpendicular (PP) configuration, three reference cases: **a** side view reference of the magnetic field N-N configuration; **b** N-S (or S-N) configuration; **c** S-S configuration

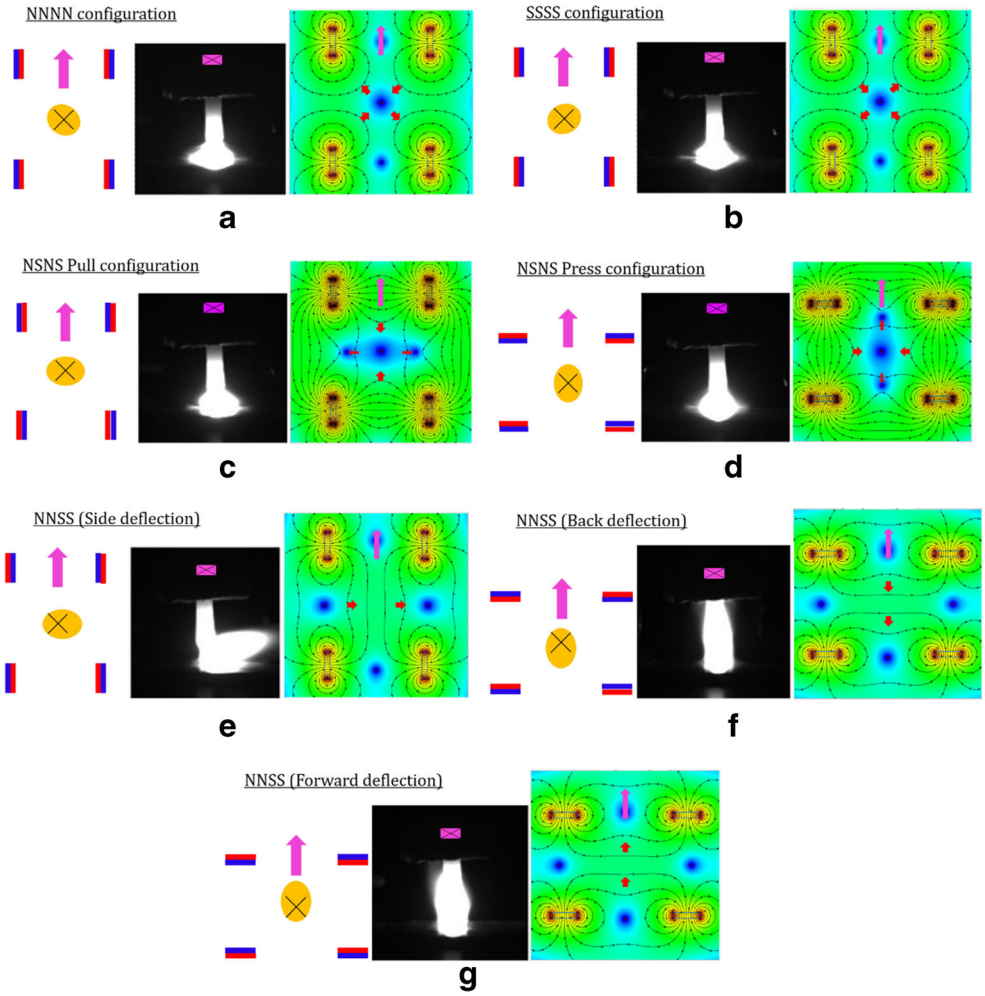

Fig. 8 The cups-type arrangement of permanent magnets, the result of the arc shape and simulation of magnetic field with predicted magnetic force in all the perpendicular (PP) configuration: **a** NNNN; **b** SSSS; **c** NSNS-Pull; **d** NSNS-Press; **e** NNSS-SD; **f** NNSS-BD; **g** NNSS-FD

of magnetic field that is measured by Gaussmeter shows that perpendicular has 97.3 mT, while parallel has 24.3 mT in the same spot location. Therefore, the welding arc is strongly deflected at perpendicular arrangement compared to the parallel arrangement.

4.2 Effect of EMF on the weld width

The appearance of the top and back bead of PP-NNSS-SD and PR-NNSS-SD configuration is shown in Fig. 9a, b. The appearance of top and back bead of PP-NNNN and PP-SSSS

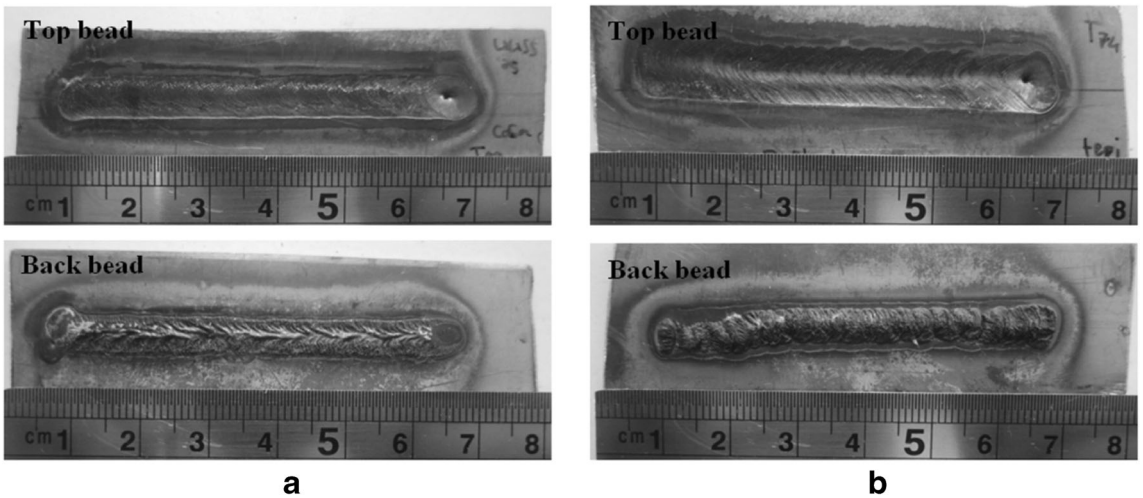

Fig. 9 Appearance of top and back bead at the configuration: **a** PP-NNSS-SD and **b** PR-NNSS-SD with $I = 80$ A and $v = 2$ mm/s

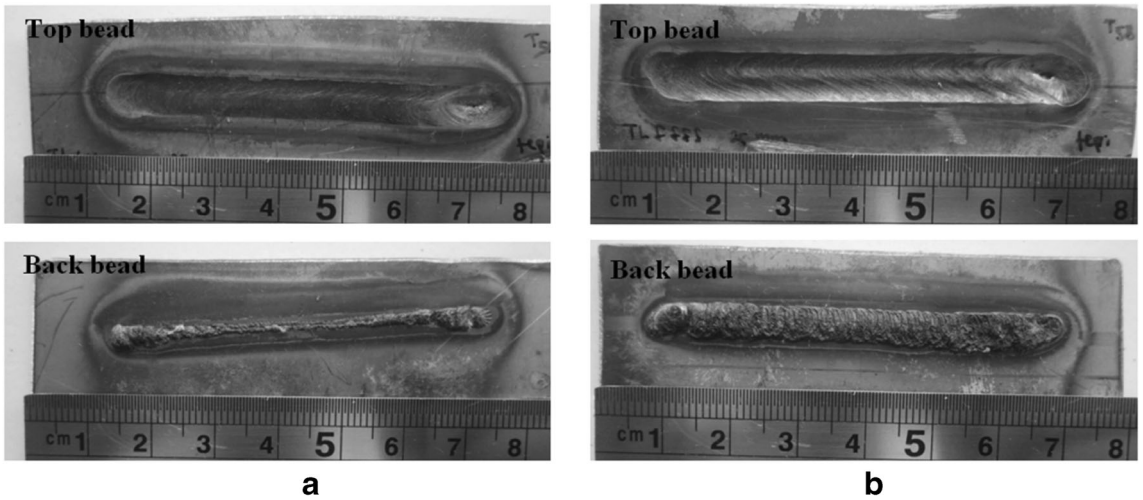

Fig. 10 Appearance of top and back bead at the configuration: **a** PP-NNNN and **b** PP-SSSS with I = 80 A and v = 2 mm/s

configuration is shown in Fig. 10a, b. The appearance of the top and back bead of PP-NSNS-Pull and PR-NSNS-Press configuration is shown in Fig. 11a, b. Figure 12a, b shows the bead width at top and back in the perpendicular (PP) and parallel (PR) arrangement of NNSS configuration. The maximum bead width achieved by using the configuration of PR-NNSS-SD where the top and back bead width are 8.32 and 5.55 mm, respectively. This configuration has significant increase as compared to the bead width of conventional TIG welding that have 6.28 mm at top bead and 5.22 mm back bead. On the other configuration, PP-NNSS-SD have resulted slightly smaller bead width than conventional TIG welding process. This is proof that the stronger magnetic field produces higher arc blow that result in the contact area of heating process in the weld pool. This corresponds to the results of several research where the higher arc blow tends to less weld penetration and more side wall penetration [7, 13]. While in the PR-NNSS-SD, the deflection of the arc increases the contact area heating process, therefore making the weld pool wider. Because of higher bend deflection while using PP arrangement, the FD and BD tend to be smaller in size of bead width compared to the PR arrangement.

Figure 13a, b shows the bead width at top and back in the perpendicular (PP) and parallel (PR) arrangement of NNNN and SSSS configuration. As shown in Fig. 13a, b, the PP-NNNN configuration has slightly increased in top bead width, while significantly decreased in back bead width. The PP-NNNN tend to have wider and shallower penetration as compared to the conventional TIG. The PP-SSSS has similar tendencies to PP-NNNN but not significant. PR-NNNN has similar results to the conventional TIG. PR-SSSS has similar results to the conventional TIG but with a smaller size in bead width. Figure 14a, b shows the bead width at top and back in the perpendicular (PP) and parallel (PR) arrangement of NSNS-Pull and NSNS-Press configuration. Theoretically, PP-NSNS-Pull has an elliptical arc stretched tangentially to the welding direction, so it will give wider weld pool. While PP-NSNS-Press and PR-NSNS-Press have an elliptical arc

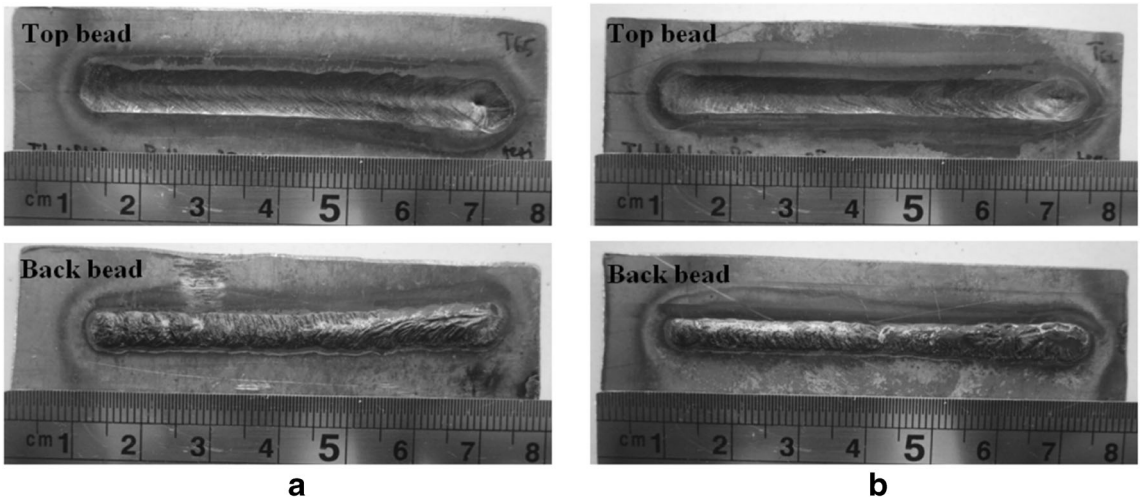

Fig. 11 Appearance of top and back bead at the configuration: **a** PP-NSNS-Pull and **b** PP-NSNS-Press with I = 80 A and v = 2 mm/s

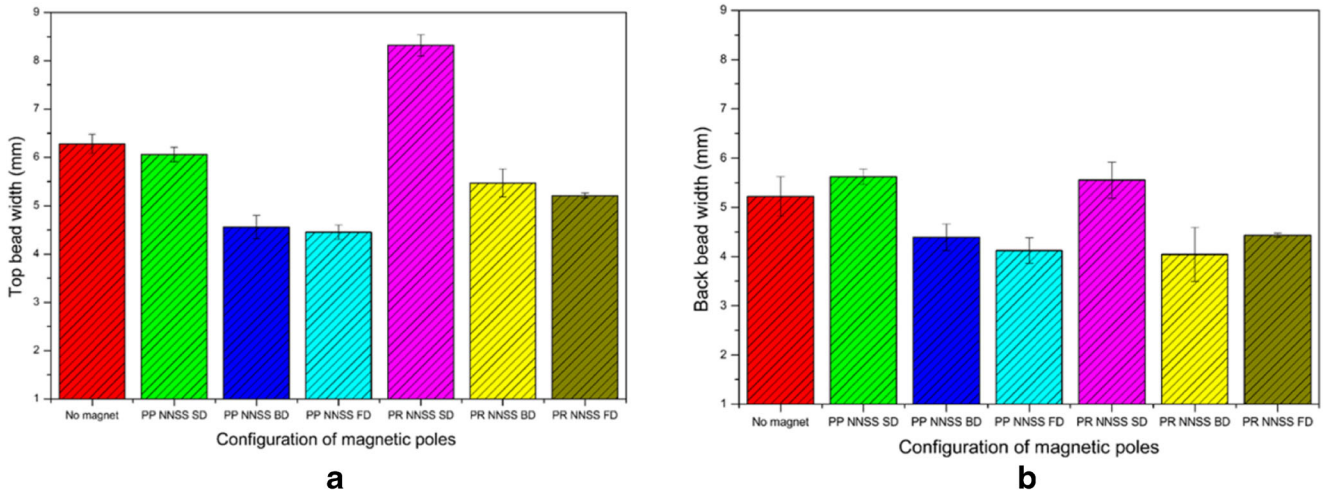

Fig. 12 The bead width **a** at top and **b** back in the perpendicular (PP) and parallel (PR) arrangement of NNSS configuration

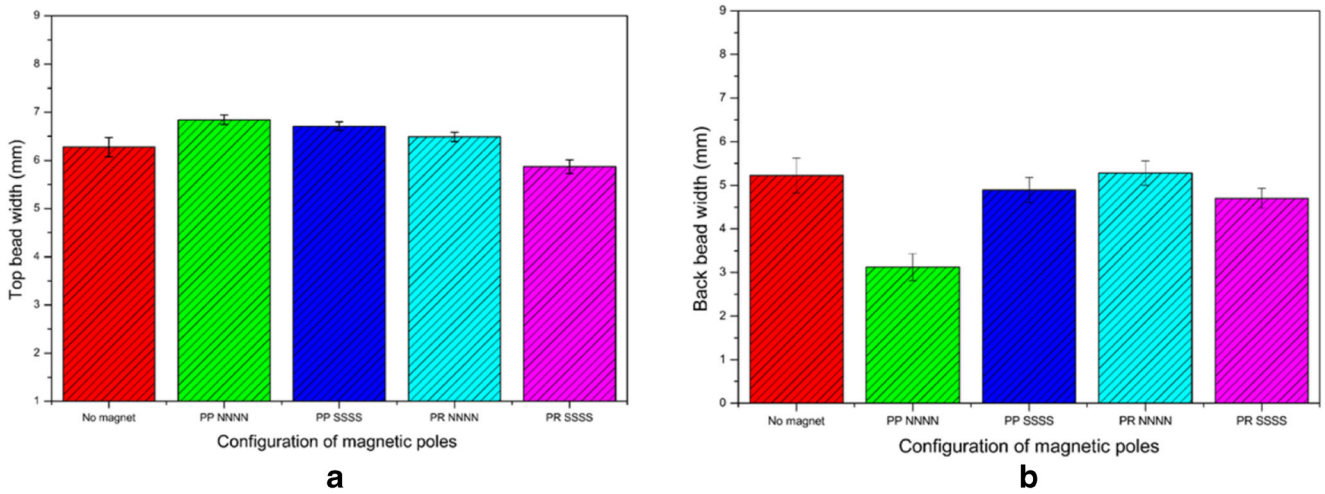

Fig. 13 The bead width **a** at top and **b** back in the perpendicular (PP) and parallel (PR) arrangement of NNNN and SSSS configuration

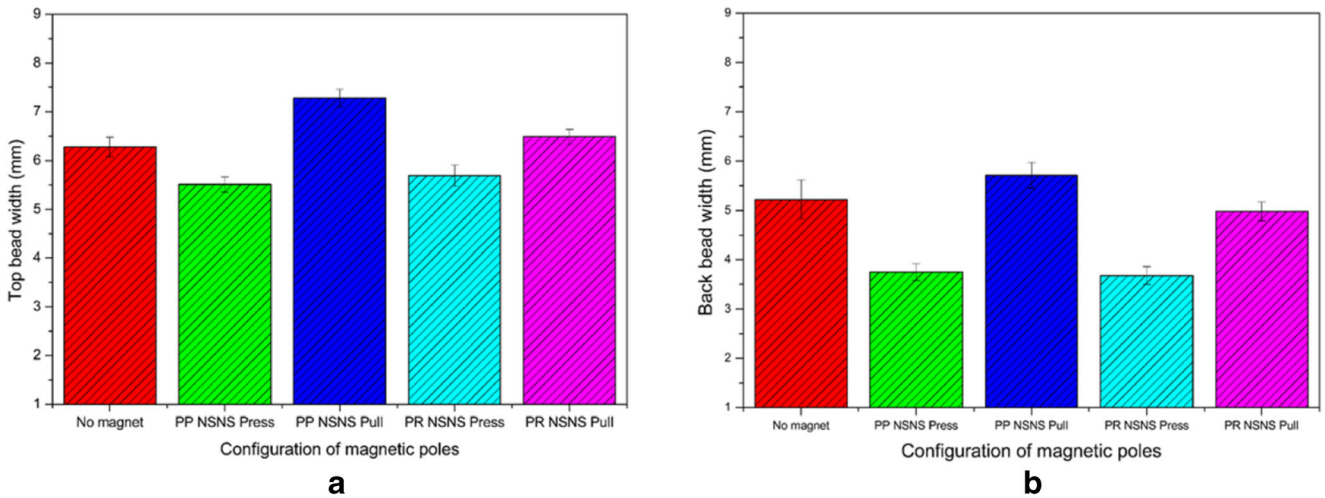

Fig. 14 The bead width **a** at top and **b** back in the perpendicular (PP) and parallel (PR) arrangement of NSNS-Press and NSNS-Pull configuration

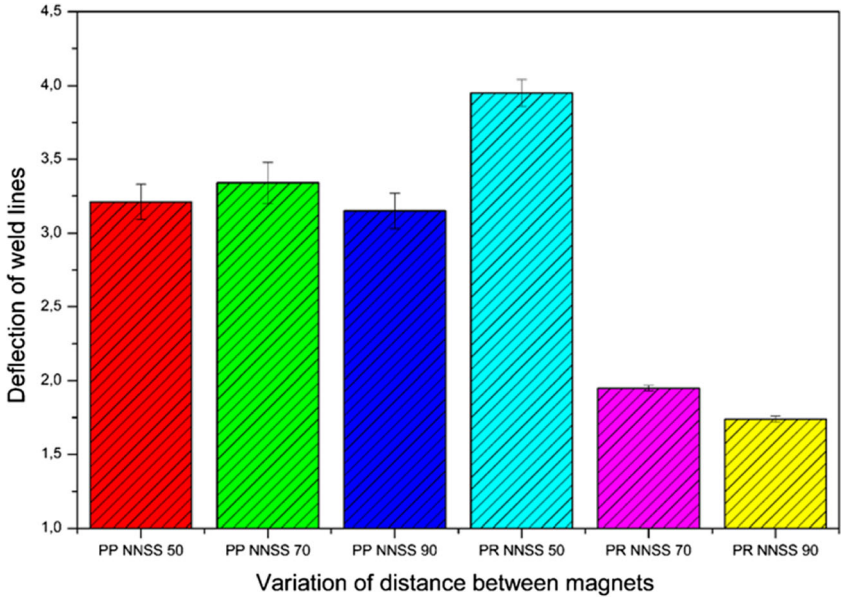

Fig. 15 The effect of distance between magnets on the deflection of the weld bead from the welding line using configuration of PP-NNSS-SD and PR-NNSS-SD

stretched normally to the welding direction, so it will give narrower weld pool. This experimental results correspond to the theoretical approach. However, PR-NSNS-Pull does not give the similar results like PP-NSNS-Pull. This is probably due to lack of magnetic field strength to produce magnetic force. Hence, it could not stretch the arc very well.

4.3 Deflection of weld lines

As shown in Fig. 15, the effect of distance between magnets on the deflection of the weld bead from the welding line using configuration of PP-NNSS-SD and PR-NNSS-SD. The variable distances used in this study are 50, 70, and 90 mm. The result shows that for PR arrangement, the deflection of weld line increased when the distance between the magnets decreased. However, the PP arrangement increased distance between magnets that have the same results of the deflection of weld line. The maximum deflection of weld line can be obtained using the configuration of PR-NNSS-SD with a distance between magnets of 50 and 3.21 mm. The possibility reason is because the area contact of welding arc on this configuration is wider; hence, the center of weld bead shifted further. The minimum deflection of weld line can be obtained using PR-NNSS-SD with 90 mm distance between magnets.

4.4 Efficiency of TIG welding process

As shown in Fig. 16, PP-NNSS-SD uses 70 and 90 mm distance between magnet achieving better results compared to the 50 mm. Because 70 or 90 mm gives less strength of magnetic field compared to the 50 mm, hence, the arc is less to bend and has more contact region for heating process, therefore

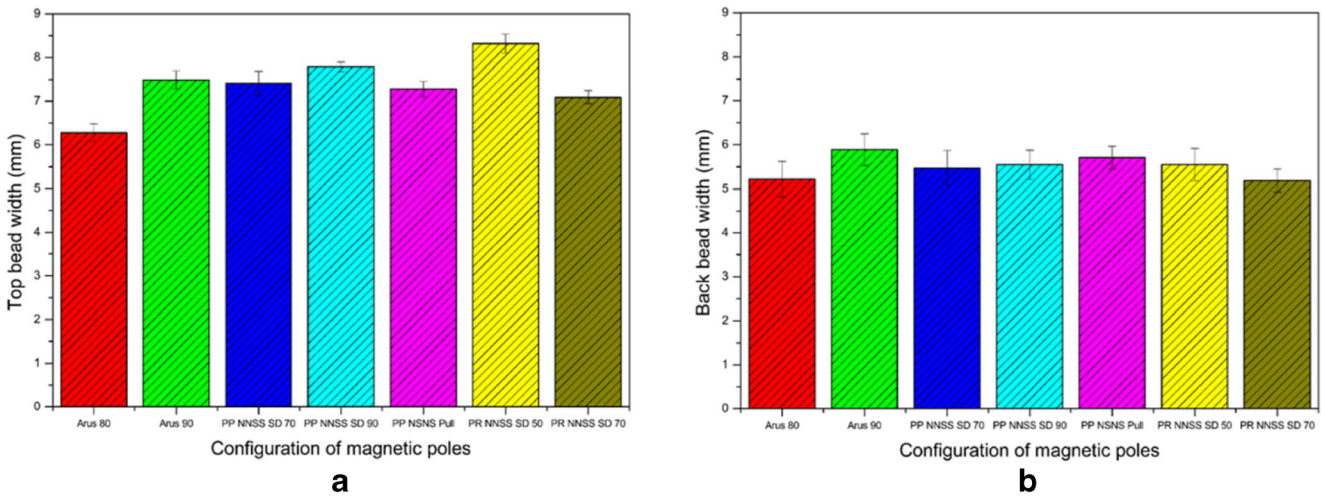

Fig. 16 Comparative result of bead width **a** at top and **b** back of PR-NNSS-SD (50 and 70 mm), PP-NNSS-SD (70 or 90 mm), or PP-NSNS-Pull (50 mm) with no magnets 80 and 90 A

increasing the weld bead width. The 90 mm distance for PP-NNSS-SD is the optimum distance, whereas the 50 mm distance is the optimum distance for PR-NNSS-SD. This attributed to the arrangement of PP produced stronger magnetic field compared to PR. However, too strong magnetic field will result in higher blow of arc and lessen the contact heating. Therefore, the optimum distance must be applied in order to generate the optimum magnetic field; hence, the optimum angle of arc blow can be achieved.

The simple comparative argument used in this paper for increasing the efficiency is using the current comparative with matching the geometry of the top and back bead width. In this case, the comparative method can only be used with a 2-mm-thick stainless steel. Hence, PR-NNSS-SD, PP-NNSS-SD, or PP-NSNS-Pull (Fig. 16) using 80 A have the equivalent result compared to the conventional welding of 90 A; this means that it reduces the power consumption up to 11% and produces almost same penetration due to the results of the back bead width. Thereby, the power efficiency is increased further.

5 Conclusions

The conclusions from this paper can be drawn as follows:

1. The PP arrangement generates a stronger magnetic field as compared to the PR arrangement.
2. The minimum deflection of weld line is PR-NNSS-SD with 90 mm distance between magnets.
3. Using an external permanent magnet, the TIG welding process using 80 A can achieve the equivalent weld geometry to the conventional TIG welding using 90 A.
4. Using PR-NNSS-SD (50 and 70 mm), PP-NNSS-SD (70 or 90 mm), or PP-NSNS-Pull (50 mm), power consumption can be reduced up to 11%; therefore, with this configuration, the efficiency is increased.
5. Therefore, PP-NNSS-SD with 90 mm distance is the best option to achieve better efficiency and minimum deflection of weld line.

Acknowledgments The authors would like to thank to Mr. Mohammad Azwar Amat, MT for the contribution in simulation work.

Funding This study was financially supported by the Directorate Research and Public Service, Universitas Indonesia through the contract number: 1753/UN2.R12/PPM.00.00/2016 with title of "Pengembangan Mesin Tungsten Inert Gas Welding Otomatis Berbasis Machine Vision dan Neural Network".

References

1. Xiao L, Fan D, Huang J (2018) Tungsten cathode-arc plasma-weld pool interaction in the magnetically rotated or deflected gas tungsten arc welding configuration. J Manuf Process 32:127–137
2. Wu H, Chang Y, Lu L, Bai J (2017) Review on magnetically controlled arc welding process. Int J Adv Manuf Technol 91(9–12): 4263–4273
3. Yin X, Gou J, Zhang J, Sun J (2012) Numerical study of arc plasmas and weld pools for GTAW with applied axial magnetic fields. J Phys D Appl Phys 45(28):285203
4. Kang YH, Na SJ (2002) A study on the modeling of magnetic arc deflection and dynamic analysis of arc sensor. Weld J (Miami, Fla) 81(1):8–13
5. Nomura K, Ogino Y, Hirata Y (2012) Shape control of TIG arc plasma by cusp-type magnetic field with permanent magnet. Weld Int 26(10):759–764
6. Baskoro AS, Tuparjono, Erwanto, Frisman S, Yogi A, Winarto (2014) Improvement of tungsten inert gas (TIG) welding penetration using the effect of electromagnetic field. Appl Mech Mater 493:558–563
7. Sun Q, Wang J, Cai C, Li Q, Feng J (2016) Optimization of magnetic arc oscillation system by using double magnetic pole to TIG narrow gap welding. Int J Adv Manuf Technol 86(1–4):761–767
8. Liu Z, Li Y, Su Y (2018) Simulation and analysis of heat transfer and fluid flow characteristics of arc plasma in longitudinal magnetic field-tungsten inert gas hybrid welding. Int J Adv Manuf Technol: 1–16. https://doi.org/10.1007/s00170-018-2320-3
9. Blais A, Proulx P, Boulos MI (2003) Three-dimensional numerical modelling of a magnetically deflected dc transferred arc in argon. J Phys D Appl Phys 36(5):488–496
10. Lin ZQ, Li YB, Wang YS, Chen GL (2005) Numerical analysis of a moving gas tungsten arc weld pool with an external longitudinal magnetic field applied. Int J Adv Manuf Technol 27(3–4):288–295
11. Li LC, Xia WD (2008) Effect of an axial magnetic field on a DC argon arc. Chin Phys B 17(2):649–654
12. Chen T, Xiaoning Z, Bai B, Xu Z, Wang C, Xia W (2015) Numerical study of DC argon arc with axial magnetic fields. Plasma Chem Plasma Process 35(1):61–74
13. Wang J, Sun Q, Feng J, Wang S, Zhao H (2017) Characteristics of welding and arc pressure in TIG narrow gap welding using novel magnetic arc oscillation. Int J Adv Manuf Technol 90(1–4):413–420
14. Li Y, Wu CS, Wang L, Gao JQ (2016) Analysis of additional electromagnetic force for mitigating the humping bead in high-speed gas metal arc welding. J Mater Process Technol 229:207–215
15. Jian L, Zongxiang Y, Keliang X (2016) Anti-gravity gradient unique arc behavior in the longitudinal electric magnetic field hybrid tungsten inert gas arc welding. Int J Adv Manuf Technol 84(1–4):647–661